MRAS Observers for Speed Estimation of Induction Motor with Direct Torque and Flux Control

Hau Huu Vo, Pavel Brandstetter and Chau Si Thien Dong

Abstract The paper describes Model Reference Adaptive System (MRAS) observers for the speed estimation of an induction motor with direct torque and flux control. The first estimator is a reference frame MRAS (RF-MRAS) and the second estimator is a current based MRAS (CB-MRAS). At first, direct torque controlled induction motor drive with two estimators are implemented on Matlab-Simulink environment. Then, comparison of two observers is done by evaluation of the rotor speed difference. The simulation results confirm that both MRAS estimators are simple to simulate and experiment. By comparison of both observers, the CB-MRAS observer gives higher accuracy of the rotor speed estimation.

Keywords RF-MRAS · CB-MRAS · Speed control · Direct torque control · Induction motor · AC drive

1 Introduction

The control and estimation of induction motor drives is almost unbounded subject, and the technology has been developing very strong in last few decades. The induction motor drive with a cage type of machine has many applications in industry such as pumps and fans, paper and textile mills, subway and locomotive

H.H. Vo (✉) · C.S.T. Dong
Faculty of Electrical and Electronics Engineering, Ton Duc Thang University,
No. 19 Nguyen Huu Tho Street, District 7, Ho Chi Minh City, Vietnam
e-mail: vohuuhau@tdt.edu.vn

C.S.T. Dong
e-mail: dongsithienchau@tdt.edu.vn

P. Brandstetter
Faculty of Electrical Engineering and Computer Science,
VSB-Technical University of Ostrava, Ostrava, Czech Republic
e-mail: pavel.brandstetter@vsb.cz

V.H. Duy et al. (eds.), *AETA 2015: Recent Advances in Electrical Engineering and Related Sciences*, Lecture Notes in Electrical Engineering 371,
DOI 10.1007/978-3-319-27247-4_29

propulsions, electric and hybrid vehicles, machine tools and robotics, home appliances, heat pumps and air conditioners, rolling mills, wind generation systems. These applications often require adjustable speed and wide power range [1, 2].

The control methods without speed encoder can be classified as follows:

- Methods with machine model [3–9]: open loop estimators, MRAS and observers (such as extended Kalman filter, Luenberger observer, sliding mode observer).
- Methods without machine model [10–14]: estimators with injection methods and estimators using artificial intelligence.

2 Modelling an Induction Motor

State-space equations of induction motor in [α, β] coordinate system can be expressed into [9] (Table 1):

Table 1 Induction motor quantities and parameters

Quantities/parameters	Value/unit	Definition
$u_{s\alpha}$, $u_{s\beta}$		Stator voltages in [α, β] coordinate system
$i_{s\alpha}$, $i_{s\beta}$		Stator currents in [α, β] coordinate system
$\hat{i}_{s\alpha}, \hat{i}_{s\beta}$		Estimated stator currents in [α, β] coordinate system
$\psi_{R\alpha}$, $\psi_{R\beta}$		Rotor fluxes in [α, β] coordinate system
$\hat{\psi}_{R\alpha}, \hat{\psi}_{R\beta}$		Estimated rotor fluxes in [α, β] coordinate system
p	2	Number of pole pairs
R_s	1.115 Ω	Stator resistance
L_m	0.2037 H	Magnetizing inductance
L_s	0.2097 H	Stator inductance
R_r	1.083 Ω	Rotor resistance
L_r	0.2097 H	Rotor inductance
T_r	0.1936 s	Rotor time constant
J	0.02 kg m^2	Moment of inertia
σ	0.0562	Total leakage constant
ω_r	rad s^{-1}	Rotor speed
T_e	Nm	Motor torque
T_L	Nm	Load torque
ξ		Adaptive signal of adaptive mechanism in MRAS structures
K_P	2000	Proportional coefficient of adaptive mechanism in MRAS structures
K_I	1,000,000	Integral coefficient of adaptive mechanism in MRAS structures

$$\frac{dX}{dt} = AX + BU_s \tag{1}$$

$$Y = X \tag{2}$$

where X, U_s, Y are the state variable vector, the input vector and the output vector, respectively as follows:

$$\begin{aligned} X &= \begin{bmatrix} i_{s\alpha} & i_{s\beta} & \psi_{R\alpha} & \psi_{R\beta} \end{bmatrix}^T \\ U_s &= \begin{bmatrix} u_{s\alpha} & u_{s\beta} \end{bmatrix}^T \end{aligned} \tag{3}$$

$$A = \begin{bmatrix} -\left(\frac{L_m^2 R_r + L_r^2 R_s}{\sigma L_s L_r^2}\right) & 0 & \frac{L_m R_r}{\sigma L_s L_r^2} & \frac{L_m \omega_r}{\sigma L_s L_r} \\ 0 & -\left(\frac{L_m^2 R_r + L_r^2 R_s}{\sigma L_s L_r^2}\right) & -\frac{L_m \omega_r}{\sigma L_s L_r} & \frac{L_m R_r}{\sigma L_s L_r^2} \\ \frac{L_m R_r}{L_r} & 0 & -\frac{R_r}{L_r} & -\omega_r \\ 0 & \frac{L_m L_r}{L_r} & \omega_r & -\frac{R_r}{L_r} \end{bmatrix} \tag{4}$$

$$B = \begin{bmatrix} \frac{1}{\sigma L_s} & 0 \\ 0 & \frac{1}{\sigma L_s} \\ 0 & 0 \\ 0 & 0 \end{bmatrix} \tag{5}$$

$$\sigma = 1 - \frac{L_m^2}{L_r L_s} \tag{6}$$

The rotor speed ω_r has relation with the torques as following equation:

$$\begin{aligned} T_e &= \frac{3}{2}\frac{L_m}{L_r} p\left(\psi_{R\alpha} i_{s\beta} - \psi_{R\beta} i_{s\alpha}\right) \\ T_e &= T_L + J\frac{d\omega_m}{dt} = T_L + \frac{J}{p}\frac{d\omega_r}{dt} \end{aligned} \tag{7}$$

3 MRAS Observers

The rotor speed can be estimated by the MRAS. First, difference between the output general quantity X_{RM} of reference model and the output general quantity X_{AM} of an adaptive or adjustable model is evaluated by adaptation mechanism. Then, this mechanism uses a controller (PI controller) for tuning the rotor speed so that the difference between X_{RM} and X_{AM} reach to zero (Fig. 1).

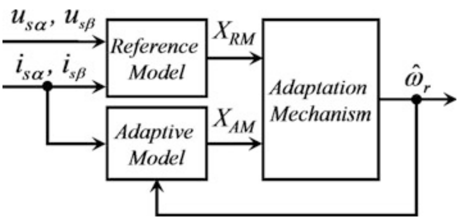

Fig. 1 MRAS structure

3.1 RF-MRAS

The structure of a reference frame model reference adaptive system (RF-MRAS) for the rotor speed estimation is shown in Fig. 2. The stator voltage and current signals are measured and used for calculating the rotor flux vector in this figure. In this model, we can get fluxes from the inputs (stator currents) only if we know the rotor speed exactly. In ideal condition, the fluxes from two models (reference and adaptive) will match. An adaptation algorithm with PI controller can be used to tune the rotor angular speed so that the adaptive signal ξ reach to zero.

The reference model is described with the following equations:

$$\psi_{R\alpha} = \frac{L_r}{L_m} \int (u_{s\alpha} - R_s i_{s\alpha}) dt - \sigma L_s i_{s\alpha} \tag{8}$$

$$\psi_{R\beta} = \frac{L_r}{L_m} \int \left(u_{s\beta} - R_s i_{s\beta}\right) dt - \sigma L_s i_{s\beta} \tag{9}$$

The adaptive model is described with the following equations:

$$\hat{\psi}_{R\alpha} = \int \left(\frac{L_m}{T_r} i_{s\alpha} - \frac{1}{T_r} \hat{\psi}_{R\alpha} - \hat{\omega}_r \hat{\psi}_{R\beta} \right) dt \tag{10}$$

$$\hat{\psi}_{R\beta} = \int \left(\frac{L_m}{T_r} i_{s\beta} - \frac{1}{T_r} \hat{\psi}_{R\beta} + \hat{\omega}_r \hat{\psi}_{R\alpha} \right) dt \tag{11}$$

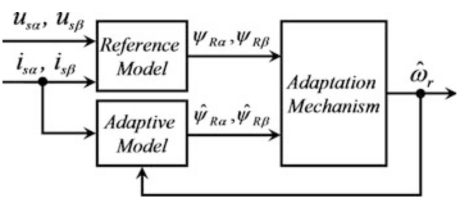

Fig. 2 Structure of RF-MRAS

Using the Popov's criterion for hyperstability for a globally asymptotically stable system, we obtain the adaptation algorithm as following equations:

$$\xi = \hat{\psi}_{R\alpha}\psi_{R\beta} - \hat{\psi}_{R\beta}\psi_{R\alpha} \tag{12}$$

$$\hat{\omega}_r = K_p\xi + K_I \int_0^t \xi dt \tag{13}$$

where $K_P > 0$, $K_I > 0$.

In practice, this method is difficult to implement, particularly at low speeds because of the pure integration of the voltage signals. The integration, however, would be subject to long-term drift in practice and special techniques should be taken to correct this drift. For example, the I-controller with the limitation can be used. Besides that, the estimation accuracy can be good if parameters of motor are constants. However, accuracy is decreased because of parameter variation.

3.2 CB-MRAS

This MRAS estimator uses output stator currents of the induction motor as output quantities of the reference model [15]. The Fig. 3 shows the structure of the CB-MRAS speed observer.

In the RF-MRAS speed observer, the voltage model is used as a reference model, and the current model is an adaptive model. In the CB-MRAS observer, the induction motor is used as a reference system, and the current model together with the current estimator are adaptive models [15].

The current estimator of CB-MRAS is described with the following equations:

$$\hat{i}_{s\alpha} = \frac{1}{T_i}\int \left(K_1 u_{s\alpha} + K_2\hat{\psi}_{R\alpha} + K_3\hat{\omega}_R\hat{\psi}_{R\beta} - \hat{i}_{s\alpha}\right)dt \tag{14}$$

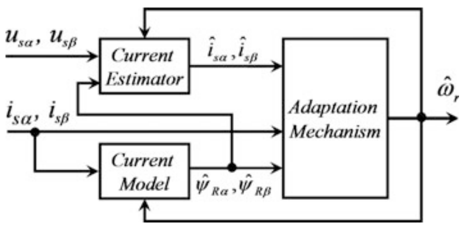

Fig. 3 Structure of CB-MRAS

$$\hat{i}_{s\beta} = \frac{1}{T_i} \int \left(K_1 u_{s\beta} + K_2 \hat{\psi}_{R\beta} - K_3 \hat{\omega}_R \hat{\psi}_{R\alpha} - \hat{i}_{s\beta} \right) dt \tag{15}$$

$$K_1 = \frac{\frac{L_r}{L_m}}{\frac{L_r R_s}{L_m} + \frac{L_m}{T_r}}; \quad K_2 = \frac{L_m}{L_r R_s T_r + L_m^2}; \quad K_3 = \frac{1}{\frac{L_r R_s}{L_m} + \frac{L_m}{T_r}}; \quad T_i = \frac{\frac{L_s L_r - L_m^2}{L_m}}{\frac{L_r R_s}{L_m} + \frac{L_m}{T_r}} \tag{16}$$

The current model of CB-MRAS is also described with the Eqs. (9)–(10). In the CB-MRAS estimator, the adaptation algorithm is different from the RF-MRAS method and is based on the error between estimated and measured stator current, according to the formula used in the full-order flux observer with speed adaptation, developed in [16, 17] (basing on the minimization of the Lyapunov function). The PI controller is also used to tune the speed as Eq. (12) with the adaption signal as the following equation:

$$\xi = \left(i_{s\alpha} - \hat{i}_{s\alpha}\right)\hat{\psi}_{R\beta} - \left(i_{s\beta} - \hat{i}_{s\beta}\right)\hat{\psi}_{R\alpha} \tag{17}$$

4 Direct Torque Control

The direct torque control (DTC) has comparable performance with the vector control. In this scheme, the torque and the stator flux are controlled directly by selecting voltage space vector of the inverter through a look up table. The block diagram of DTC is shown in Fig. 4. Firstly, this techniques compare the command torque and stator flux with estimated values. Then, the errors will be processed by hysteresis-band controllers.

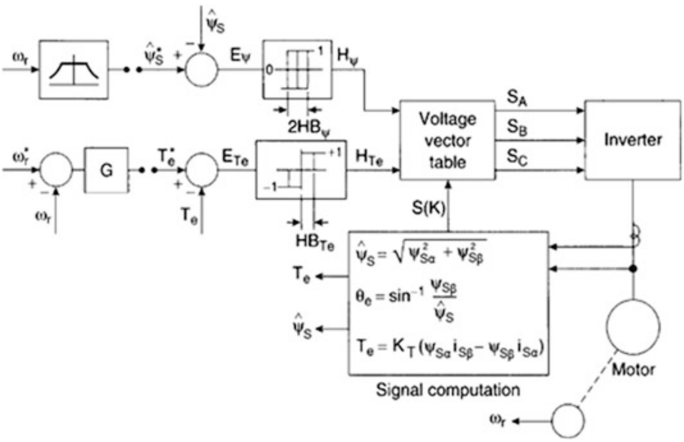

Fig. 4 Block scheme of the direct torque control

High performance control, such as vector control or direct torque control, is based on a dynamic model of the induction motor expressed in a stationary coordinate system or rotating coordinate system which is oriented on the rotor magnetic flux vector.

The flux controller has two levels:

$$\begin{aligned} H_{\psi} &= 1 \;\text{ for }\; E_{\psi} > +HB_{\psi} \\ H_{\psi} &= -1 \;\text{ for }\; E_{\psi} < -HB_{\psi} \end{aligned} \tag{18}$$

The torque controller has three levels:

$$\begin{aligned} H_{Te} &= 1 \;\text{ for }\; E_{Te} > +HB_{Te} \\ H_{Te} &= -1 \;\text{ for }\; E_{Te} < -HB_{Te} \\ H_{Te} &= 0 \;\text{ for }\; -HB_{Te} < E_{Te} < +HB_{Te} \end{aligned} \tag{19}$$

The signal computation block (see Fig. 4) calculates signals from the voltage model of the induction motor. This block also seeks where stator flux vector lies (see Fig. 5).

DTC technique has some special features:

- no feedback current control,
- no traditional PWM algorithm,
- no vector transformation,

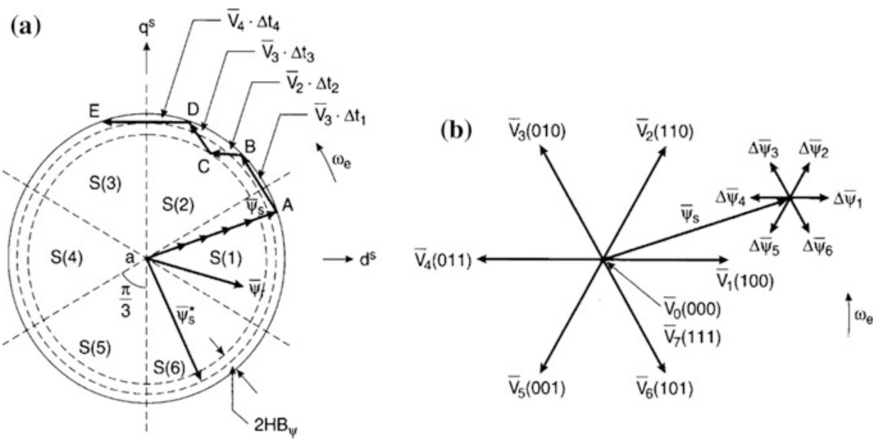

Fig. 5 **a** Trajectory of the stator flux vector in DTC control. **b** Inverter voltage vectors and corresponding flux variation in time Δt

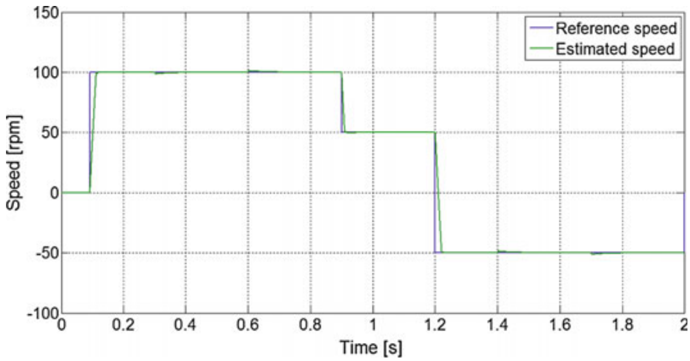

Fig. 6 RF-MRAS, reference speed (*blue*) and estimated speed (*green*)

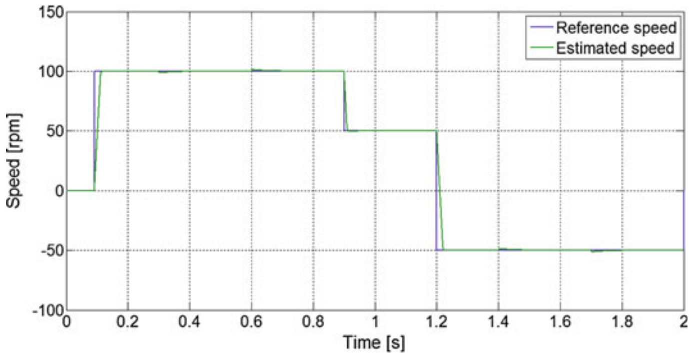

Fig. 7 CB-MRAS, reference speed (*blue*) and estimated speed (*green*)

- feedback signal processing is similar to stator flux-oriented vector control,
- hysteresis-band controller generates flux and torque ripple and switching frequency is not fixed (like hysteresis-band current control) (Figs. 6 and 7).

5 Simulation Results

The described induction motor drive was simulated using Matlab-Simulink. The time courses of important quantities were obtained from the control structure with two observers at the jump of the load torque $T_L = 2$ Nm (see Figs. 10 and 11). The simulation results showed that the speed difference (see Figs. 8 and 9) and torque ripple (see Figs. 10 and 11) of the CB-MRAS were smaller than those of the RF-MRAS.

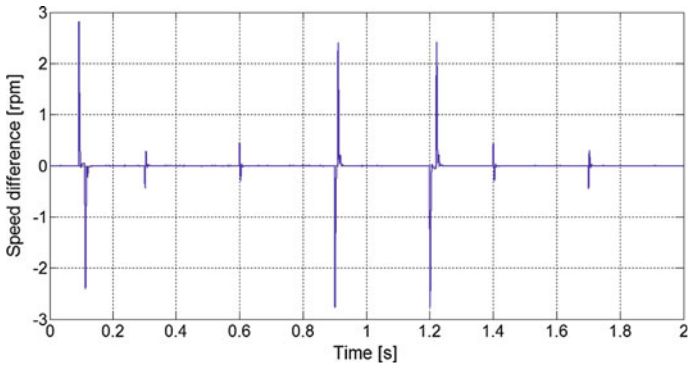

Fig. 8 RF-MRAS, difference between real speed and estimated speed

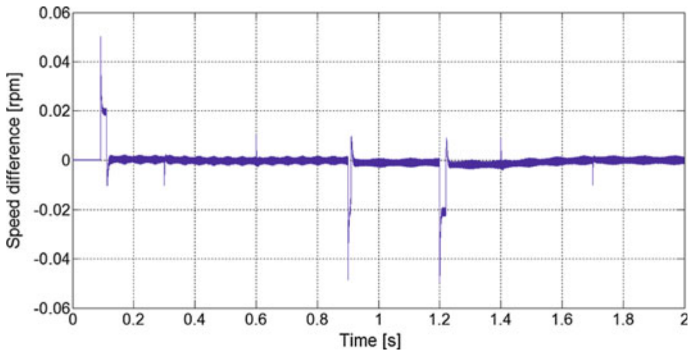

Fig. 9 CB-MRAS, difference between real speed and estimated speed

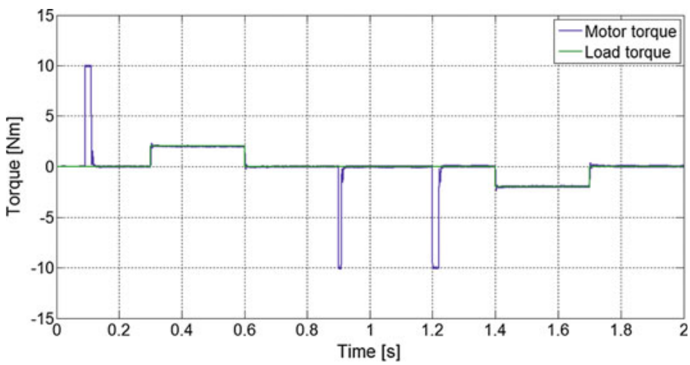

Fig. 10 RF-MRAS, motor torque (*blue*) and load torque (*green*)

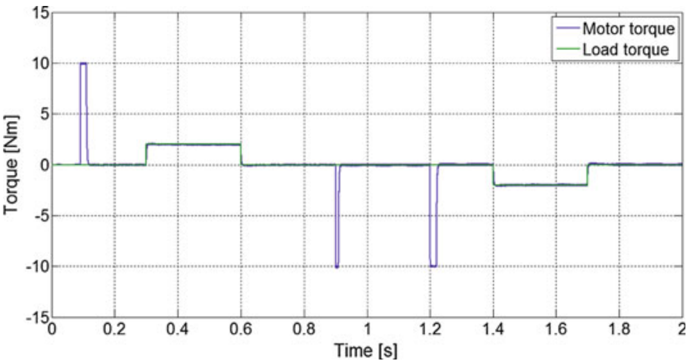

Fig. 11 CB-MRAS, motor torque (*blue*) and load torque (*green*)

6 Conclusion

The estimation technique for sensorless induction motor drive with the direct torque control was presented in the paper. The speed estimator was based on application of the MRAS observers. The induction motor drive with two MRAS estimators gave good dynamic responses and the estimation of the mechanical speed was good in steady state and also in transient state. The CB-MRAS observer gave higher accuracy of the rotor speed estimation than the RF-MRAS observer. This MRAS estimator could be used for rotor speed estimation without speed encoder in the control system with digital signal processor.

Acknowledgments The paper was supported by the projects: IT4Innovations Centre of Excellence project, reg. no. CZ.1.05/1.1.00/02.0070 funded by the European Regional Development Fund and the national budget of the Czech Republic, and project reg. no. SP2015/81 funded by the Student Grant Competition of VSB-Technical University of Ostrava.

References

1. Holtz J (2002) Sensorless control of induction motor drives. Proc IEEE 90(8):1359–1394
2. Vas P (1998) Sensorless vector and direct torque control. Oxford University Press, Oxford
3. Gacho J, Zalman M (2010) IM Based speed servodrive with luenberger observer. J Electr Eng 61(3):149–156
4. Salvatore N, Caponio A, Neri F, Stasi S, Cascella GL (2010) Optimization of delayed-state Kalman-Filter-Based Algorithm via differential evolution for sensorless control of induction motors. IEEE Trans Industr Electron 57(1):385–394
5. Sutnar Z, Peroutka Z, Rodic M (2010) Comparison of sliding mode observer and extended Kalman filter for sensorless DTC controlled induction motor drive. In: Conference Proceedings, 14th International Power Electronics and Motion Control Conference (EPE/PEMC), pp T7-55–T7-62

6. Haron AR, Idris NR (2006) Simulation of MRAS-based speed sensor-less estimation of induction motor drives using MATLAB-SIMULINK. In: The First International Power and Energy Conference PECon, Putrajaya, Malaysia, pp 411–415
7. Lascu CH, Boldea I, Blaabjerg F (2006) Comparative study of adaptive and inherently sensorless observers for variable-speed induction-motor drives. IEEE Trans Ind Electron 53 (1):57–65
8. Consoli A, Scarcella G, Bottiglieri TA (2006) Harmonic analysis of voltage zero-sequence-based encoderless techniques. IEEE Trans Ind Appl 42(6):1548–1557
9. Sbita L, Ben Hamed M (2007) An MRAS – based full Order Luenberger observer for sensorless DRFOC of induction motors. ICGST ACSE J 7(1):11–20
10. Partal S, Senol I, Bakan AF, Bekiroglu KN (2011) Online speed control of a brushless AC servomotor based on artificial neural networks. Turk J Electr Eng Comput Sci 19(3):373–383
11. Gadoue SM, Giaouris D, Finch JW (2009) Sensorless control of induction motor drives at very low and zero speeds using neural network flux observers. IEEE Trans Ind Electron 56 (8):3029–3039
12. Kouzi K, Nait-Said MS, Hilairet M, Berthlot E (2009) Fuzzy MRAS speed estimator for vector control of an induction motor. Int Rev Electr Eng (IREE) 4(2):278–283
13. Perdukova D, Fedor P (2007) Fuzzy model based control of dynamic system. JEE-J Electr Eng 7(3):5–11, ISSN 1582-4594
14. Ma T-T (2010) Adaptive inverse control schemes based on fuzzy neural networks for induction motor drives. Int Rev Electr Eng (IREE) 5(4):1563–1570
15. Orlowska-Kowalska T, Dybkowski M (2010) Stator-current-based MRAS estimator for a wide range speed-sensorless induction-motor drive. IEEE Trans Ind Electron 57(4):1296–1308
16. Kubota H, Matsuse K, Nakano T (1993) DSP-based speed adaptive flux observer of induction motor. IEEE Trans Ind Appl 29(2):344–348
17. Kubota H, Matsuse K, Nakano T (1990) New adaptive flux observer for wide speed range motor drives. In: Proceedings of IEEE-IECON, pp 921–926